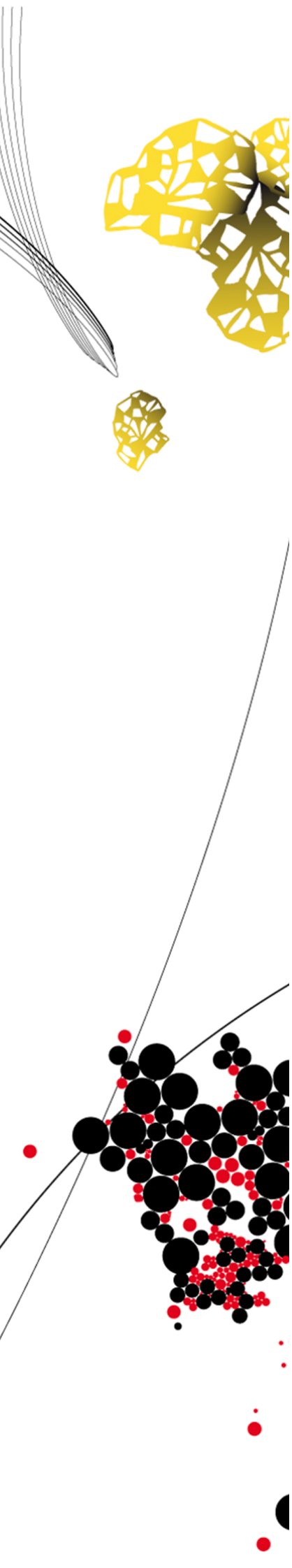

UNIVERSITY OF TWENTE.

Faculty of Electrical Engineering, Mathematics & Computer Science

# Reducing the dynamic range of analog-to-digital converter in FMCW harmonic radars

**Askar Sadykov**

**BSc.** Thesis **July 2024**

**Supervisors**
**University of Twente:**

Dr. Anastasia

Lavrenko

Andrei Mogilnikov

Radio Systems Group
Faculty of Electrical Engineering, Mathematics and Computer Science
University of Twente
P.O. Box 217
7500 AE Enschede
The Netherlands

# Summary

Frequency Gain Control (FGC), an equivalent of Sensitivity Time Circuit (STC) in Frequency-Modulated-Continuous-Wave (FMCW) radars, stands for applying a highpass filter (HPF) with the slope matching the negative slope of the path loss to the beat signal, given direct relation of its frequency to the target range. This technique primarily takes care of two issues: ground clutter and saturation of the receiver. In harmonic FMCW radars, the ground clutter is resolved by separating the receiver from the transmitter by frequency. Nevertheless, the problem of saturation remains. Apart from preventing the saturation of the receiver, FGC can reduce the dynamic range of the analog-to-digital converter (ADC), allowing for lower resolution of the ADC. In radars, due to the path loss, the magnitude of the received signal coming from further distances can be smaller than the quantization step of the ADC at the receiver's side. To be able to detect the target at such distances, the resolution must be high. The primary goal of this research was to reduce the dynamic range of the ADC with the help of FGC, to allow for a cheaper ADC with lower resolution. This paper provides the methodology and the results of the computer simulations in Matlab that show how FGC affects the power of the received signal for a harmonic FMCW radar. Also, a comparison to a conventional FMCW radar is made. This research shows that applying FGC to ease the ADC resolution requirement successfully restricts the power of the received signal to a level that does not exceed the ADC's dynamic range. This paper argues that, for linear radars, a second-order HPF should be used. And for harmonic systems, third-order characteristics apply for low-power applications, whereas for high-power applications, a second-order filter with the calibration of the cut-off frequency is a better choice.

# Contents

# Chapter 1

# Introduction

Frequency-modulated continuous-wave radar is a short-range radar that uses continuous waves, whose frequency is modulated in the transmitter [1]. FMCW radar systems use the concept of intermediate frequencies, and the distance to the target is obtained using the frequency response of the intermediate-frequency signal. This signal is obtained by mixing the transmitted signal with the received signal in the receiver chain [1].
There is a specific type of FMCW radar, a so-called harmonic FMCW radar. The main feature of this design is that the EM wave is transmitted at the fundamental frequency in the forward link (FL) and at its second harmonic in the backward link (BL).
For instance, [2] presents two low-cost and mobile prototypes of such radar systems that operate in the S-band and in the X-band. The application of this radar is to track insects in the short range. The conversion to a second harmonic here is done with a small tag placed on the insects.
Frequency Gain Control (FGC) is an important technique used in such radar systems to tackle various issues related to the principles of operation. In most applications, FGC is used to mitigate the effect of ground clutter. Due to free space propagation losses (FSPL), the reflections from nearby objects, especially the ground, are much stronger than the reflections from the designated target located much further. As a result of this factor, the receiver can get saturated by a very strong reflected signal. With the use of FGC, signals related to closer distances are attenuated. The frequency of the intermediate-frequency (IF) signal is directly proportional to the distance to the target [1]. By attenuating the frequencies related to closer distances, the effect of ground clutter can be minimized. Numerous researches have looked into this subject. A study by [3] presented a solution that prevents the saturation of the receiver due to ground clutter. Also, they went even further and applied this technique to the detection of buried objects. In a nutshell, the main idea is that the received signals are attenuated with respect to the path loss, which is proportional to $d^{-4}$ for power, with $d$ being the distance to the target. Since $d$ is directly proportional to the frequency of the IF signal $f_b$, a highpass filter with a certain slope can be used. For $f_b^{-4}$, a 40 dB/decade transition band of the filter is used in this research. Another research

by [4] also comes up with an FGC approach for FMCW radars. In their Ku-band receiver, they used a high pass filter characteristic with the transition band inversely proportional to $f_b^{-4}$. For harmonic radars, ground clutter is resolved by separating reception from the transmission by frequency. Therefore, FGC is not needed for this purpose.

Nevertheless, the usage of FGC is not limited to clutter, and other challenges can be considered in this context. For example, to maximize the range of operation, one has to use a high-resolution ADC. A high-resolution ADC will help to span the whole dynamic range of the signal, from the strongest signal to the weakest based on the distance to the target. With low resolution, the lowest possible signal can be lower than the quantization step and therefore will become undetectable. FGC can help to reduce the dynamic range of the received signal by attenuating closer ranges. Then, a lower-resolution ADC can be used.

The catch is that at low incident power levels, such a tag exhibits non-linear behavior, and, for larger distances, the path loss is now proportional to $d^{-6}$ [2], [5]. This poses some challenges in using FGC in harmonic FMCW radars because different HPF configurations need to be considered.

This paper will give an overview of linear and harmonic FMCW radars and dive into what affects the dynamic range of the ADC in these systems. Then, this paper will discuss how FGC can help to reduce the required dynamic range for both linear and harmonic radars. Also, the type of filters for harmonic radars will be specified. Matlab computer simulations will be used to verify the effectiveness of FGC in this application, as well as they will help to compare the performance of this technique between linear and harmonic cases.

# Chapter 2

# FMCW radars

## 2.1 FMCW linear radar

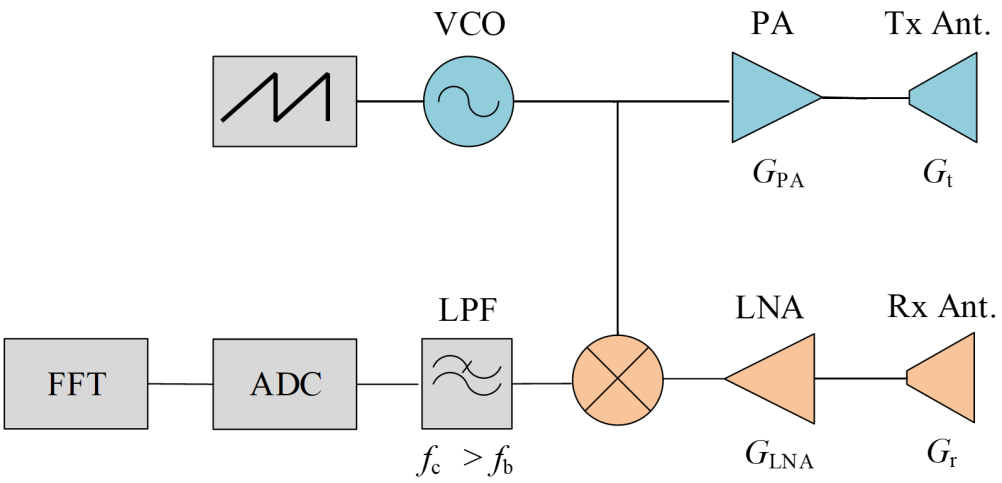


**Figure 2.1:** A block diagram of the linear FMCW radar.

The working principle of any FMCW radar lies in emitting a frequency-modulated waveform. The carrier wave is modulated by a chirp, which is, simply put, a linear growth of frequency against time. The chirp can be described with two variables: the frequency sweep $B$ or the bandwidth of the chirp, and the chirp duration $T_c$ [6]. An illustration can be seen in figure 2.2.

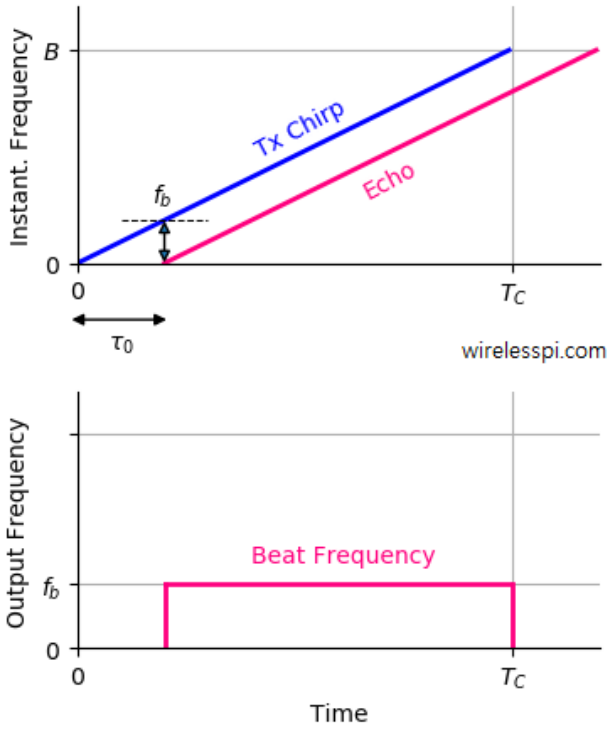


**Figure 2.2:** An illustration of the chirp and the echoes of this chirp (top picture). The resulting beat frequency after downconversion (bottom picture). [6]

For these parameters, the transmitted signal $s(t)$ with the power $P_{Tx}$, and the carrier frequency $f_{ca}$ can be represented with the following equation:

$$s(t) = \sqrt{2P_{Tx}}cos(2\pi f_{ca}t + \frac{B}{T_c}t^2 - 0.5Bt) \tag{2.1}$$

The received signal with power $P_{Rx}$ can be written in the following way:

$$r(t) = \sqrt{2P_{Rx}}cos(2\pi f_{ca}t + \frac{B}{T_c}(t - T_p)t - 0.5Bt) \tag{2.2}$$

This signal has lost its power due to propagation loss and has a propagation delay $T_p$. Therefore, its frequency differs from the transmitted signal. At the receiver, the signal is fed into a frequency mixer along with the signal at the transmitter. The mixer in this application is designed to subtract the frequencies of both signals. The output of the mixer, the IF signal, therefore, has its own frequency, called the beat or IF frequency. The IF signal is given in equation 2.3:

$$y(t) = \sqrt{2P_y}cos(\frac{B}{T_c}T_p t) \tag{2.3}$$

The beat frequency is then equal to:

$$f_b = \frac{B}{T_c}T_p = \frac{B}{T_c}\frac{2d}{c} \tag{2.4}$$

As can be seen, the frequency of this signal is proportional to the target range $d$. $c$ is the speed of light. Thus, the distance to the target can be approximated by obtaining the frequency of the IF signal. Practically, this can be achieved using the Fast-Fourier transform (FFT) due to its low computational complexity [4]. To use FFT, the signal has to be first digitized, so an ADC has to be used.

The power of the signal varies with range, so to obtain the relation between the transmitted power and the received power, one has to use Friis' equation for the wavelength $\lambda$, which implies a one-way transmission between the transmitter and the receiver:

$$P_{Rx} = P_{Tx}G_{Tx}G_{Rx}(\frac{\lambda}{4\pi d})^2 \tag{2.5}$$

In any radar applications, the transmitter emits an electromagnetic (EM) waveform and the receiver listens to the reflections from the supposed target. The target, in this case, can be seen as a reflector. The power reflected by the target can be expressed as:

$$P_{reflected} = P_{Tx}G_{Tx}\frac{\sigma}{4\pi d^2} \tag{2.6}$$

Where $\sigma$ is the radar cross-section (RCS) with the units of area.

To get the expression of the power at the receiver, one has to additionally account for the gain of the receiver's antenna and the path loss related to the way back, assuming that the receiver is located at the same spot as the transmitter.

$$P_{Rx} = P_{Tx}G_{Tx}\frac{\sigma}{4\pi r^2}(\frac{\lambda}{4\pi d})^2 G_{Rx} = P_{Tx}G_{Tx}G_{Rx}\frac{\lambda^2}{(4\pi)^3 d^4} \tag{2.7}$$

## 2.2 FMCW Harmonic radar

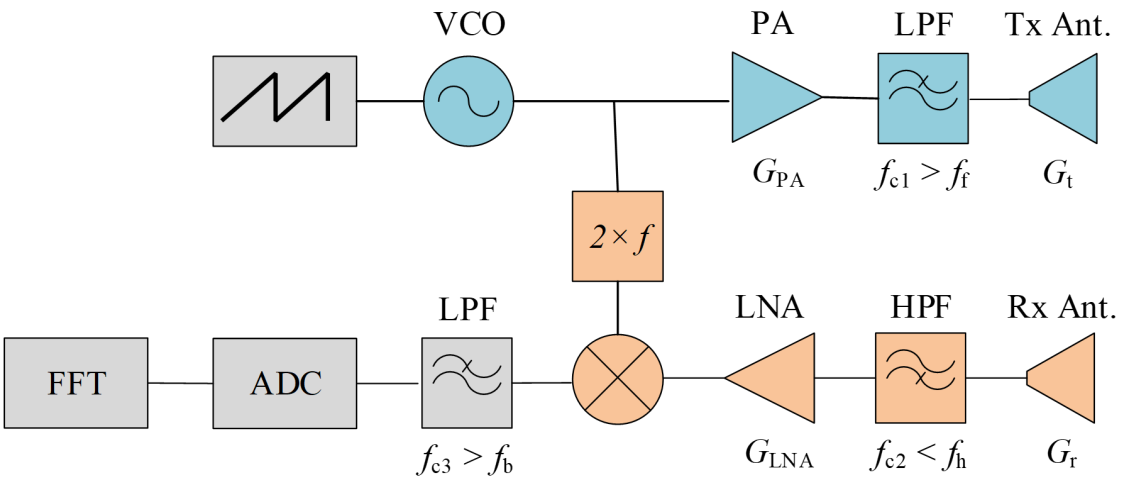


**Figure 2.3:** A block diagram of the harmonic FMCW radar.

The main difference of the harmonic radar is that instead of just a target that reflects the incident EM waves, the system's utilization requires placing a small harmonic tag on the target object. In the case of the insect tracking application, such a tag has to be lightweight and small in size to fit on the insect. For that reason, this tag purely consists of passive elements [2].

The prior goal of the tag is to convert the incident EM wave at the fundamental frequency to its second harmonic and send back the converted wave to the receiver.

The photo of the tag can be seen in figure 2.4. Shortly put, it is a wire-based dipole antenna with an inductive loop and a low-voltage diode connected in parallel to the loop [7].

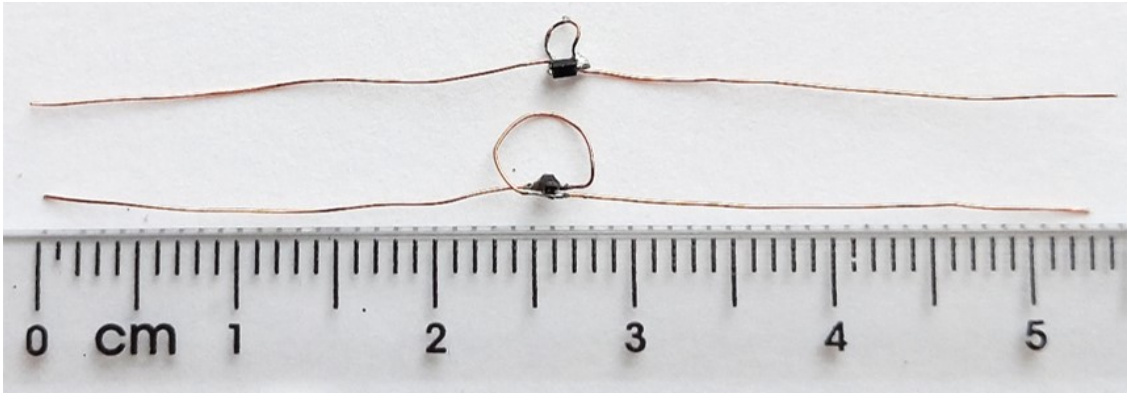


**Figure 2.4:** A photo of the harmonic tag, that is simulated in this research.

The main metric of the tag's performance evaluation is the conversion efficiency defined by:

$$\eta_H = \frac{P_{out,2f_0}}{P_{in,f_0}} \tag{2.8}$$

$P_{in,f_0}(P_{in})$ is the input power to the tag at the fundamental frequency, and $P_{out,2f_0}(P_{out})$ is the output power at the second harmonic.

At low incident power levels, the conversion factor $\eta_H$ exhibits non-linear behaviour and becomes approximately quadratic [5]:

$$P_{out,2f_0} = \eta_H P_{in,f_0}^2 \tag{2.9}$$

So, [5] presents a two-region tag model. The linear region is described by the large-signal model of the tag, and the quadratic region by the small-signal model.

The plot of the output power against the input power for the harmonic tag can be seen in figure 2.5.

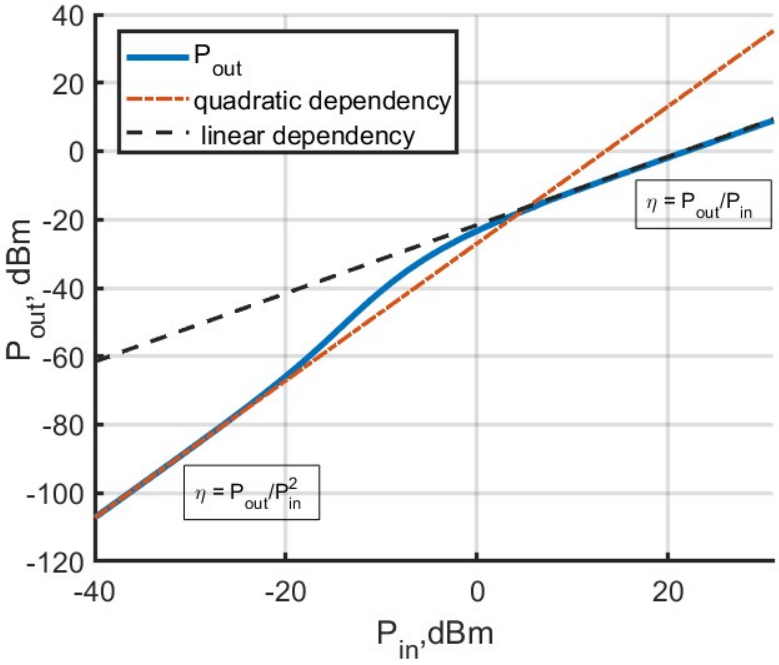


**Figure 2.5:** $P_{out}$ vs. $P_{in}$ of the harmonic tag. Here, two regions are presented: with linear dependency (large-signal model) and quadratic dependency (small-signal model), excluding the transition between them .

The main deviation from the path loss equation of the conventional radar is due to a different target model. Now, the waveform is not reflected by the target, but received by the tag's antenna, converted to second harmonic, and then re-radiated by the same antenna [7]. This requires to change the representation of the RCS of such a target. Below a table of notations is presented for this section [2].

| | |
|---|---|
| $P_{Tx}$ | Transmitted power at the fundamental frequency |
| $P_{HRX}$ | Received power at second harmonic |
| $G_{Tx}$ | Gain of the transmitting antenna |
| $G_{FRX}$ | Gain of the tag's antenna at the fundamental frequency |
| $G_{HTX}$ | Gain of the tag's antenna at the second harmonic |
| $G_{Rx}$ | Gain of the receiving antenna |
| $\lambda_F$ | Fundamental wavelength |
| $\eta_H$ | Conversion efficiency of the tag |

**Table 2.1:** Notations for this section [2]

The relation of $P_{Rx}$ to $P_{Tx}$ is given by [2] :

$$P_{Rx} = P_{Tx} G_{FTX} (\frac{\lambda_F}{4\pi r})^2 G_{FRX} \eta_H G_{HTX} (\frac{0.5\lambda_F}{4\pi d})^2 = \frac{1}{4} G_{FTX} G_{HRX} \frac{\lambda_F^2}{(4\pi)^3 d^4} \sigma_H \tag{2.10}$$

[7] introduces a so-called cross-section of the harmonic tag:

$$\sigma_H = G_{FRX} G_{HTX} \frac{\lambda_F^2}{4\pi} \tag{2.11}$$

Equation 2.9 presents some complications to the equation2.7. At some ranges, the equation will obtain the following form [2]:

$$P_{HRX} = \frac{1}{4} P_{FTX}^2 G_{FTX}^2 G_{FRX} \frac{\lambda_F^4}{(4\pi)^5 d^6} \sigma_H \tag{2.12}$$

The received power curve will be proportional to $d^{-4}$ for shorter ranges and to $d^{-6}$ for longer ranges. The former corresponds to the large-signal model, and the latter corresponds to the small-signal model of the tag [5]. Therefore, for convenience, these two regions on the received power curve will be referred to as the large-signal region and the small-signal region.

# Chapter 3

# Frequency Gain Control

## 3.1 Input dynamic range

The dynamic range of the ADC (DR) is the relation of minimum and maximum power that the receiver can process. The maximum power can defined by the signal power at the smallest distance of the radar's operation range, which depends on the application of this radar. The minimum power that can be processed is determined by the hardware of the receiver. The dynamic range of the ADC can be expressed in the following form:

$$DR = \frac{V_{max}}{V_{min}} = \sqrt{\frac{P_{Rx,max}}{P_{Rx,min}}} \tag{3.1}$$

In this equation, $P_{Rx,max}$ and $P_{Rx,min}$ stand for the maximum and the minimum received power respectively, that the radar can process. $V_{max}$ and $V_{min}$ for the corresponding magnitudes of the IF signal.

The power of the IF signal for the gain of the receiver's front-end $G_{fe}$, which includes the hardware pass-losses, gains of LNA, HPF, mixer, and LPF (Fig. 2.3). is given as [8]::

$$P_y = G_{fe} P_{Rx} \tag{3.2}$$

In the radar itself, the filter has to be implemented in the baseband. And the dynamic range of the ADC, is the dynamic range of the IF signal. However, that brings another parameter to the analysis - $G_{fe}$ For simplicity, all the simulations will be performed on the received signal instead of the IF signal. Since the power of the IF signal is directly proportional to the power of the received signal (Eq. 3.2), such an assumption will hold.

The resolution of the ADC for a given dynamic range DR in dB scale is given as:

$$\frac{A_{max}}{A_{min}} \leq 2^N \tag{3.3}$$

$$20log_{10}(2^N) = 20log_{10}(DR) \tag{3.4}$$

$$N = \frac{DR_{dB}}{6.02} \tag{3.5}$$

The required DR for the ADC will increase for higher power budgets if one wants to increase the total range of operation. Since DR is defined by the ratio of $P_{Rx,max}$ and $P_{Rx,min}$, larger transmit power $P_{Tx}$, and larger gains of the transmitting and receiving antennas, $G_{Tx}$ and $G_{Tx}$, put larger requirements on the ADC's DR.

## 3.2 Reduction of the dynamic range with FGC

The idea of FGC is the following: DR can be reduced by constraining the maximum power of the received signal. Equation 2.4 shows the relation of the target's range d with the beat frequency $f_b$ of the IF signal. These two parameters are linearly proportional, which enables one to draw the link between $P_{Rx}$ and $f_b$:

$$P_{Rx} \propto f_b^{-4} \tag{3.6}$$

Thus, one can find the frequency at which $P_{Rx}$ drops to the certain value that we want to constrain the signal to. The power level $P_{DR}$, to which the IF signal has to be constrained, can be found as:

$$P_{DR,dBm} = P_{min,dBm} + DR_{dB} \tag{3.7}$$

This equation is given in logarithmic scale and emerges from the equation 3.1. Figure 3.1 illustrates the curve of $P_{Rx}$ with respect to $f_b$ and additionally shows the power restriction $P_{DR}$ required for a certain DR of the ADC.

The intersection of $P_{DR}$ and $P_{Rx}$ will take place at a certain $f_b$. Then, for the lower frequencies, the received power will exceed the maximum allowed power level. Therefore, the lower frequencies will be attenuated by an HPF to fit within the constraint. That $f_b$, at which the intersection occurs, will be the cut-off frequency $f_{cut-off}$ of the HPF.

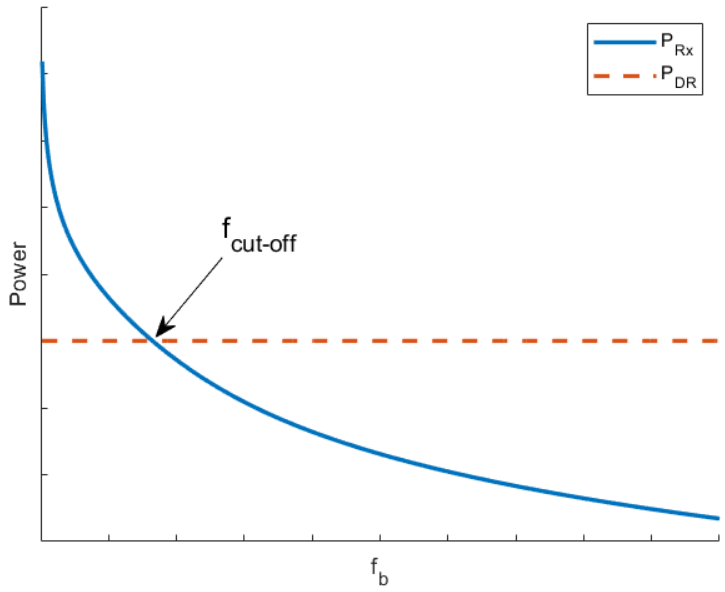


**Figure 3.1:** The illustration of how the cut-off frequency for the HPF is obtained.

The primary objective is to not let $P_{Rx}$ exceed $P_{DR}$, but the signal in that frequency range should not be attenuated too much. Ideally, it is preferred to keep the signal power exactly on the restriction level $P_{DR}$ before the cut-off frequency. This is easily achievable for the linear radar, whereas for the harmonic radar, the solution is more non-trivial due to the non-linearity of the tag.

### 3.2.1 Linear radar

In linear radars, the power loss rate is always equal to - 40dB/decade corresponding to the path loss proportional to $d^{-4}$ [3] (see eq. 2.7). To compensate, the slope of the HPF should be exactly the opposite of that of the propagation loss. This approach is illustrated in figure 3.2.

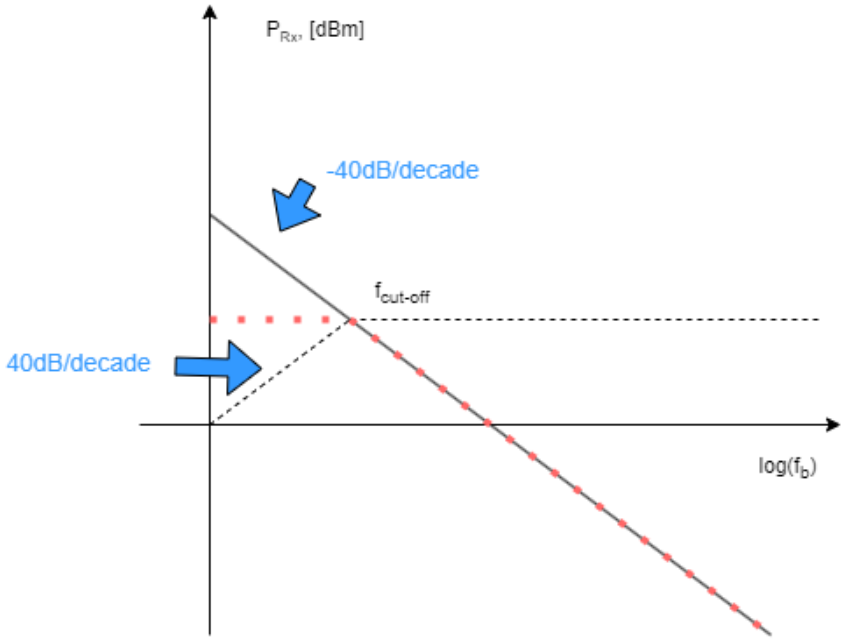


**Figure 3.2:** Illustration of how the power of the signal is restricted by an HPF for linear radars. The slope of the filter, opposite to the slope of the path loss for the received power ensures that the power level before $f_{cut-off}$ is the same.

### 3.2.2 Harmonic radar

For the non-linear case, a 60dB/decade slope will be required if the incident power of the tag is low because the path loss slope of $P_{Rx}$ in the frequency domain in the small-signal region is:

$$P_{Rx,dBm} = 10log_{10}(\alpha f_b^{-6}) + 30 = -60log_{10}(\alpha f_b) + 30 \tag{3.8}$$

Given that $\alpha$ is a constant. The transition band of a third-order filter can be used to get this slope. However, the 60dB/decade slope works only for certain distances, since the non-linear behavior of the tag is apparent at low incident power levels, and is linear otherwise [5]. For the HPF, a 60dB/decade or a 40dB/decade can be used solely, but sacrificing overall efficiency. In the former case, the shortest ranges will be attenuated more than they should, and in the latter, the shorter ranges will not be attenuated enough, and the received power will overshoot. In this case, calibration of the cut-off frequency will be required.

The calibration procedure involves finding the new cut-off frequency for the HPF that would simply align the 40dB/decade slope of $P_{Rx}$ with the maximum allowed power level $P_{DR}$. Such frequency would be higher than the previously obtained frequency for the solution based on a third-order filter characteristic. The process of the cut-off frequency's calibration is given in figure 3.3

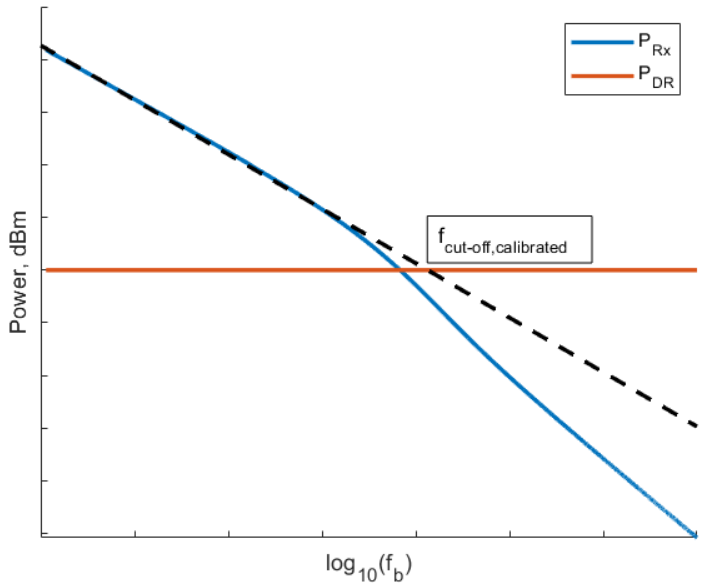


**Figure 3.3:** This figure illustrates how the cut-off frequency is calibrated to use a second-order filter. The large-signal region is extended, and its intersection with $P_{DR}$ shows the new cut-off frequency. In this case, the large-signal region will perfectly align with the max. allowed level after filtering.

As can be seen, the large region is extended until it reaches $P_{DR}$ at the new frequency. An HPF with this frequency set as the cut-off frequency will perfectly align the 40dB/decade region of the $P_{Rx}$ curve with $P_{DR}$, and the signal power will not overshoot.

Both of these methods will be tested since the transition between the large-signal and the small-signal region depends on the system's power characteristics. As was mentioned before, the non-linearity of the tag can be observed for certain incident power levels. So, if the transmitted power, or the gain of the transmitting antenna changes, the position of this transition on the power curve also changes. Therefore, these two approaches are likely to perform differently in different power conditions.

# Chapter 4

# Results

## 4.1 Simulation setup

As a reference for the fixed hardware, the S-band prototype from [2] will be taken. The parameters of this system are given in table 4.1. We used a model of a harmonic tag containing a wire half-wavelength dipole with a Schottky diode model SMS7630-079LF [9].

Knowing the maximum distance of detection, we can determine the minimum received power level, which can still be read by the receiver.

Figure 4.1 shows the graph of $P_{Rx}$ for this harmonic S-band prototype. The maximum range of this radar is 40 m [2].

| Frequency (fundamental/harmonic), GHz | 2.9/5.8 |
|---|---|
| Frequency sweep, MHz | 80 |
| Sweep time, ms | 1 |
| Transmitted power, $P_{FTX}$, dBm | 34 |
| Tx antenna gain, dBi | 13 |
| Rx antenna gain, dBi | 14 |
| Maximum detected range, m | 40 |

**Table 4.1:** System specifications for the S-band prototype [2]

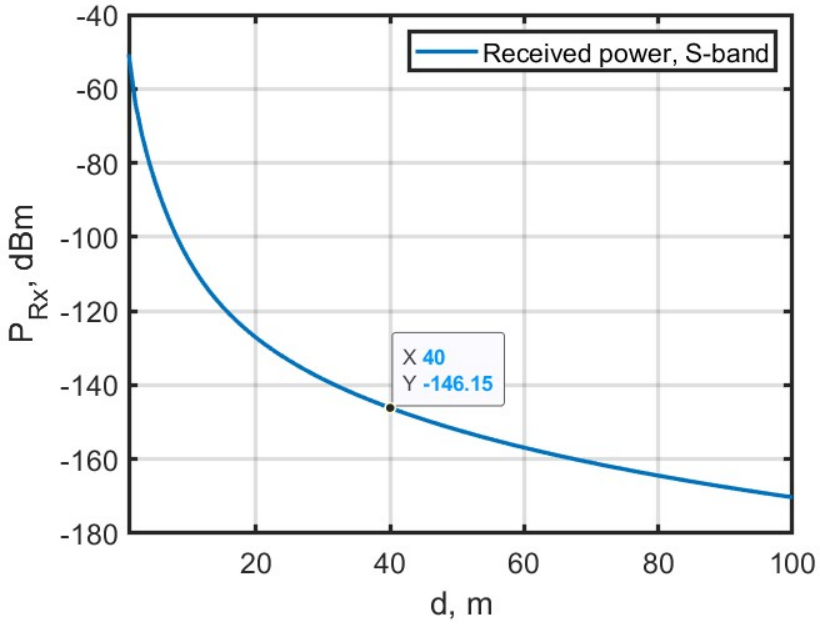


**Figure 4.1:** $P_{Rx}$ curve of the S-band prototype. At the maximum distance of 40m, the minimum power that the receiver can read is pointed.

As can be seen from the graph, the received power at this distance is -146.15 dBm. So, $P_{min}$ is -146.15 dBm. As can be seen from the figure 4.1, the power at the receive antenna port is equal to -146.15 dBm when the harmonic tag is at a distance of 40 m from the transmitter. Since the power of the IF signal is directly proportional to the power of the received signal 2.4, we are going to use this value as our reference for the minimum received power $P_{min}$.

## 4.2 Filter Design

There are a lot of tools in Matlab that can be used for filter design. For this application, a Butterworth HPF was used, the advantage of which is the flat pass band. In Matlab, it is convenient to use the 'butter(N,$f_{cut-off}$,'type')' function. N corresponds to the filter order, $f_{cut-off}$ to the normalized cut-off frequency, and 'type' the type of the filter, in this case a highpass ('high') [10].

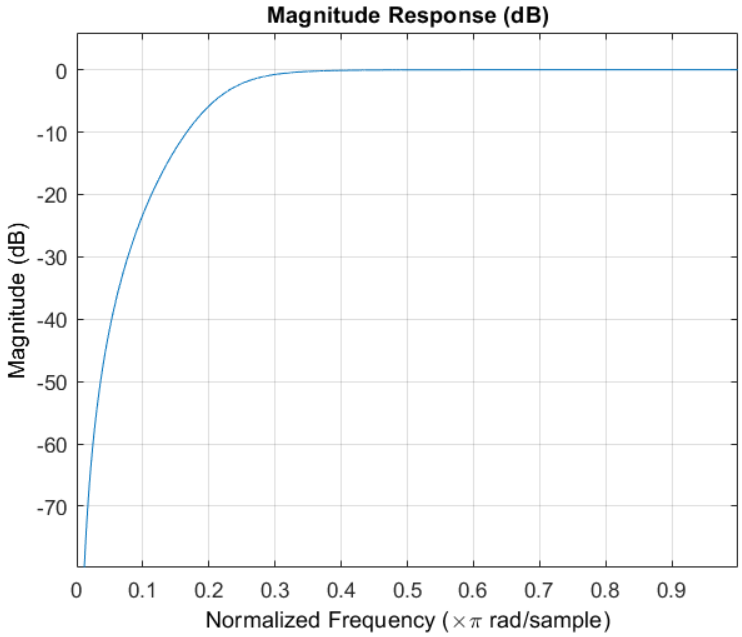


**Figure 4.2:** The magnitude response of a third-order Butterworth filter with a cut-off frequency of 0.5B, where B is the bandwidth of the chirp. The sampling frequency for this filter is 4B

This is a digital IIR filter, so the analog cut-off frequency has to be converted to the normalized frequency, with respect to the sampling frequency. The sampling frequency should be chosen as at least twice the bandwidth of the IF signal, according to the Nyquist theorem. That ensures that the transfer function of the filter will be used correctly.

The transfer function is needed for efficiency since the signals are not to be sampled and filtered in the time domain. Such simulations would be very time-consuming. Instead, the transfer function for this filter will be derived and simply used on the power curves:

$$P_{Rx,filtered}(f_b) = |H(j2\pi f_b)|^2 P_{Rx}(f_b) \tag{4.1}$$

To obtain a transfer function of a digital filter in Matlab, 'freqz(b,a,N)' function should be used, where b,a are the filter coefficients, and N is the number of digital frequency samples in the filter given in rad/sample from 0 to $\pi$.

### 4.2.1 Linear radar.

The dynamic range is dependent on several parameters, namely $P_{Tx}$,$G_{Tx}$,$G_{Rx}$,$\sigma$. Radar-cross-section $\sigma$ is fixed to a value of 20 $mm^2$, corresponding to an RCS of a honey bee [11]. The motivation for this value comes from the need to compare the harmonic radar to the linear one. The given harmonic tag is used for tracking insects, so the linear radar should be put into similar conditions.

Figure 4.3 shows the relation of DR with respect to the transmitted power given different values of the antennae gains: $G_{Tx,1}$ = $G_{Rx,1}$ = 15 dBi, $G_{Tx,2}$ = $G_{Rx,2}$ = 25 dBi. Figure 4.3 shows the required number of bits for the same power level expressed in these parameters. The maximum received power for the calculation of DR is taken at the distance of 1m.

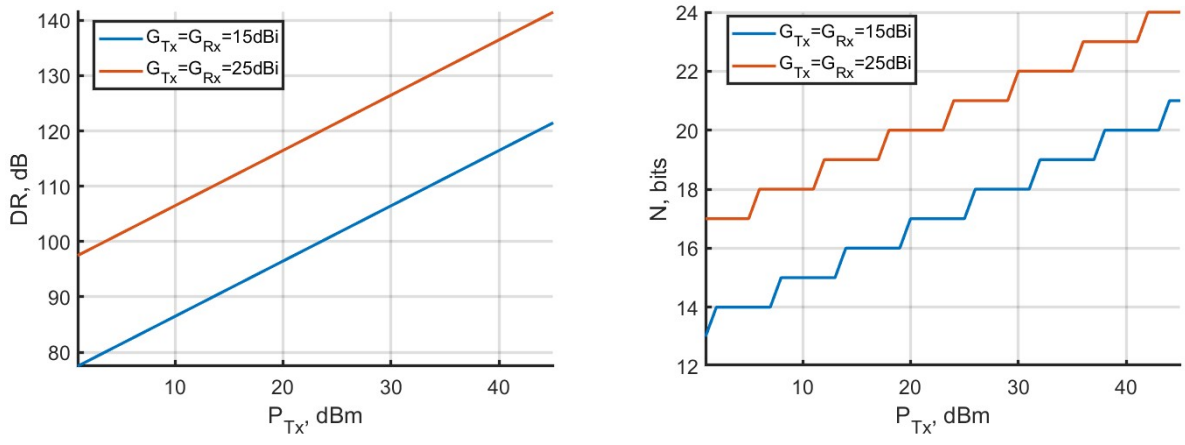


a) b)

**Figure 4.3:** The dynamic range of the IF signal with respect to the transmitted power in the linear radar (a). The corresponding required resolution for these dynamic ranges(b)

As can be observed, a large value of power and the antennas' gains put a high requirement on the ADC's resolution, yet improving the maximum target range.

Let's see how DR is correlated with the maximum target range. The target range will be obtained for certain power budgets presented in table 4.2.

| $P_{Tx}$, dBm | $G_{Tx} = G_{Rx}$, dBi |
|---|---|
| 25 | 15 |
| 35 | 15 |
| 45 | 15 |
| 25 | 25 |
| 35 | 25 |
| 45 | 25 |

**Table 4.2:** Values of transmitted power and gains of receive an transmit antennas used in the simulations

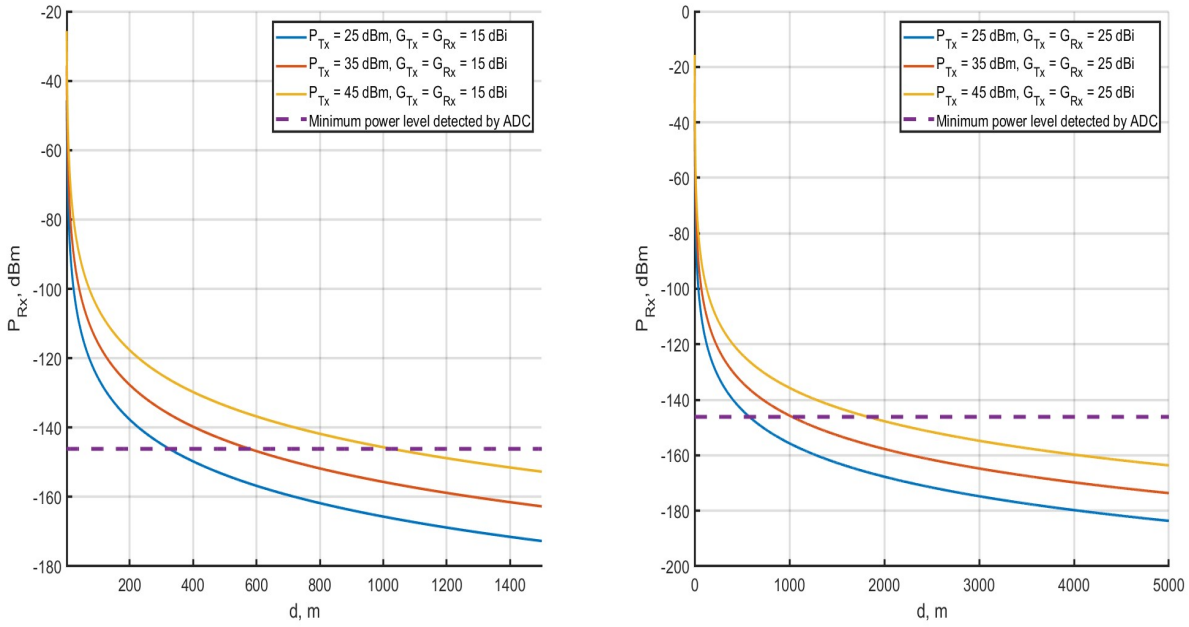


a) b)

**Figure 4.4:** The received power with respect to the distance to the target for different transmitted power an antenna gains - 15dBi(a), 25dBi(b). Also, the minimum power level is readable by the receiver. The intersection of the received power curve and the minimum level is the max. operational range for a certain power budget. Linear radar.

| $P_{Tx}$, dBm | $G_{Tx} = G_{Rx}$, dBi | DR, dB | N, bits | max. range, m |
|---|---|---|---|---|
| 25 | 15 | 101.479 | 17 | 319 |
| 35 | 15 | 111.479 | 19 | 588 |
| 45 | 15 | 121.479 | 21 | 1089 |
| 25 | 25 | 121.479 | 21 | 1089 |
| 35 | 25 | 131.479 | 22 | 1910 |
| 45 | 25 | 141.479 | 24 | 3383 |

**Table 4.3:** Parameters, and the corresponding DR, resolution, and the maximum operation range for the linear system.

For the given desired resolution, we can now derive the constraint on the dynamic range. Three values for the resolution will be taken: 8,10,12 bits. Using the equation 3.5, we can compute:

$$DR_8 = 6.02 * 8 = 48.18dB \tag{4.2}$$

$$DR_{10} = 6.02 * 10 = 60.20dB \tag{4.3}$$

$$DR_{12} = 6.02 * 12 = 72.24dB \tag{4.4}$$

Figure 4.5 shows the relation of the beat frequency of the IF signal $f_b$ to the dynamic range DR required for it for the linear radar. In the same figure, the DR levels corresponding to the given ADC resolutions are given. The intersections with the DR curves indicate where the cut-off frequency of HPF should be. Below, in table 4.4, the cut-off frequencies for HPF given for a certain power budget are provided. As can be seen, the cut-off frequencies grow with the growth of power in the system. A higher resolution, to the contrary, makes the cut-off frequency smaller, since the constraint on DR is weaker.

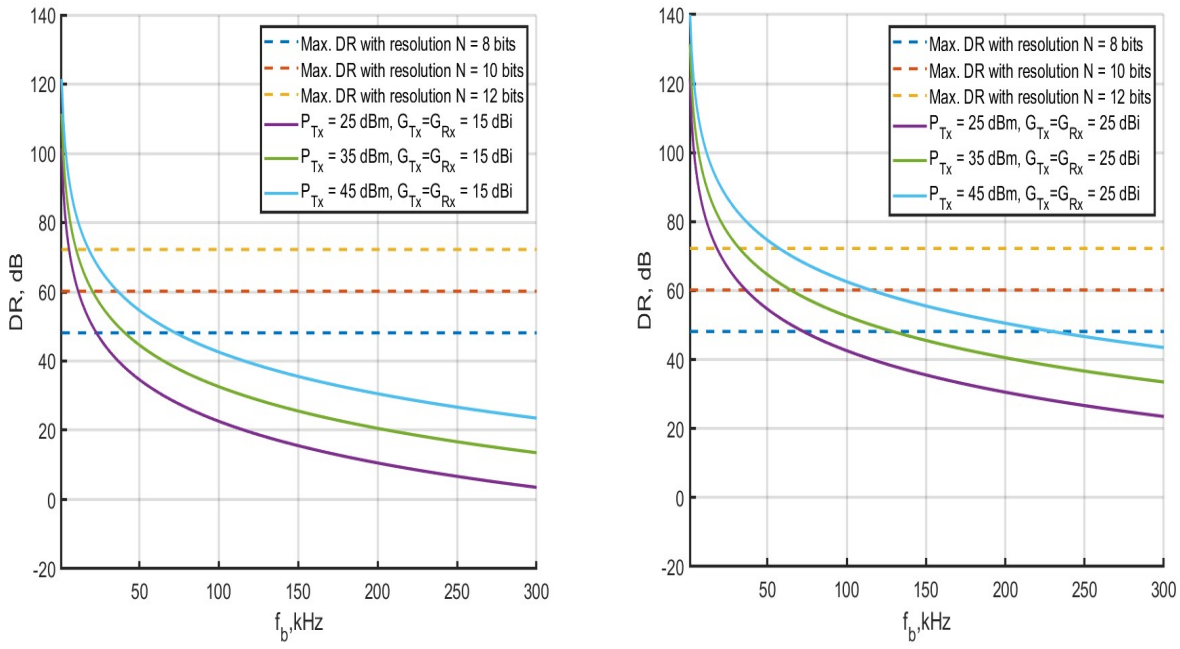


**Figure 4.5:** Relations of dynamic ranges versus beat frequency for systems with different transmitted power and antenna gains 15 dBi (a) and 25 dBi (b). The maximum power levels for 8,10,12 bits. The intersections of these levels with the dynamic ranges indicate the cut-off frequencies for HPFs. Linear radar

| Power budget \ Resolution, bits | 8 | 10 | 12 |
|---|---|---|---|
| $P_{Tx} = 25dBm, G_{Tx} = G_{Rx} = 15dBi$ | 11.20 | 5.87 | 2.67 |
| $P_{Tx} = 35dBm, G_{Tx} = G_{Rx} = 15dBi$ | 20.27 | 10.13 | 5.34 |
| $P_{Tx} = 45dBm, G_{Tx} = G_{Rx} = 15dBi$ | 36.27 | 18.14 | 9.07 |
| $P_{Tx} = 25dBm, G_{Tx} = G_{Rx} = 25dBi$ | 36.27 | 18.14 | 9.07 |
| $P_{Tx} = 35dBm, G_{Tx} = G_{Rx} = 25dBi$ | 64.00 | 32.50 | 16.00 |
| $P_{Tx} = 45dBm, G_{Tx} = G_{Rx} = 25dBi$ | 114.67 | 57.07 | 28.80 |

**Table 4.4:** The cut-off frequencies derived for the linear radar, given for a certain resolution and power budget.

Now, that the frequencies are known, the designed filter can be applied to the linear radar. To see how such a filter would affect $P_{Rx,linear}$ with respect to the beat frequency, we can simply generate a vector of $P_{Rx,linear}$ for a range of distances, and generate a frequency vector using equation 2.4. The filter order should be set to 2, and the cut-off frequency should be taken from table 4.4.

In figure 4.6, the outcome of the filter's application is shown. The figure shows the results for the ADC resolution of 10 bits and 3 power budgets: $P_{Tx}$ is given as 25,35,45 dBm with the gains of the antennas equal to 15 dBi.

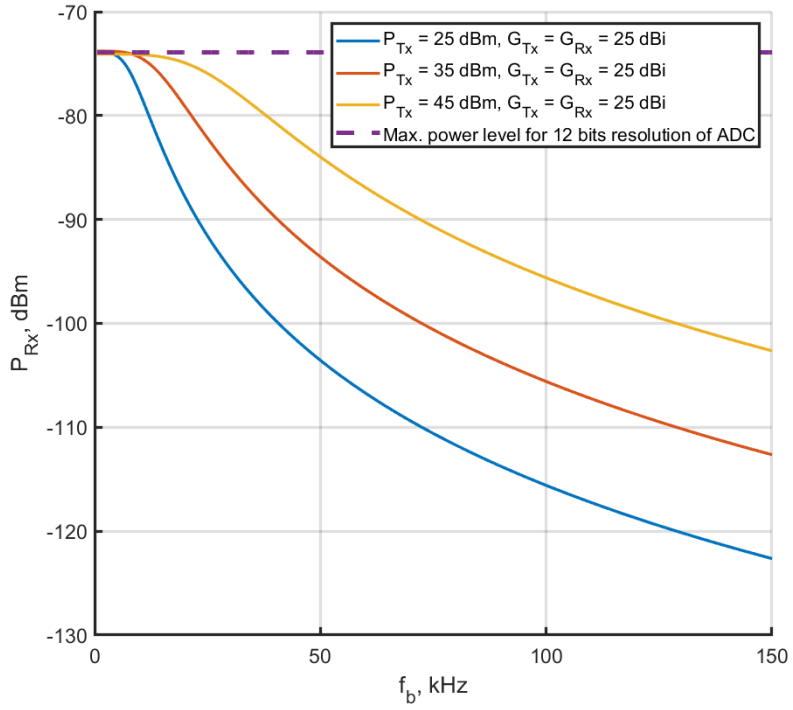


**Figure 4.6:** The received power for 12-bit resolution of the ADC and the antenna gains of 25 dBi after applying an HPF.

The following behavior can be outlined: up to the cut-off frequency the power of the signal remains constant at the level defined by what DR should be.

### 4.2.2 Harmonic radar.

With regards to the relation of the dynamic range to the power budget represented by $P_{Tx}$, $G_{Tx}$, $G_{Rx}$, the harmonic radar follows the same tendency as its linear equivalent. The only difference is that the slope of the DR curve changes for higher power. This is the influence of the non-linearity of the harmonic tag's conversion efficiency at low incident power levels. For higher power, the slope changes because the behavior of the conversion tag becomes linear again.

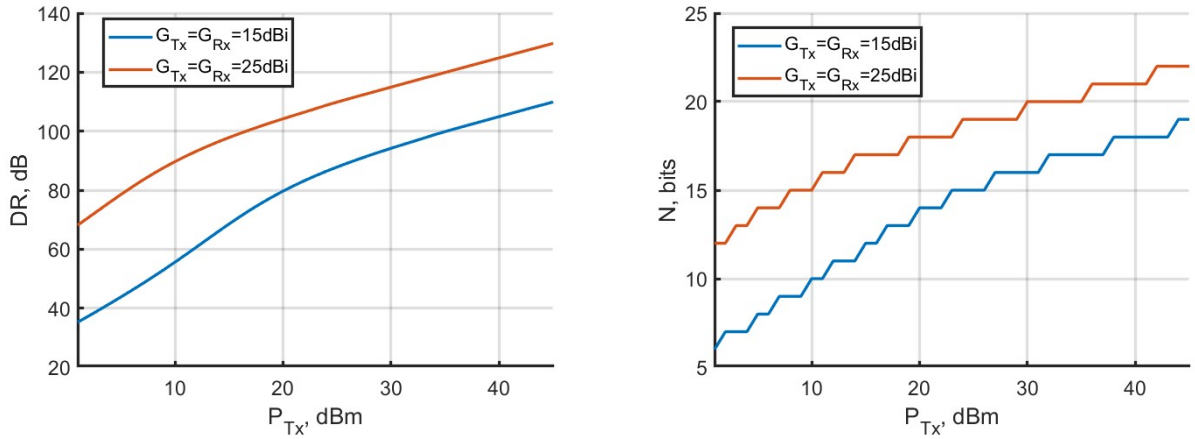


**Figure 4.7:** The dynamic range of the IF signal with respect to transmitted power for different antenna gains (15,25 dBi) in the harmonic radar (a). The corresponding required resolution for these dynamic ranges(b)

Overall, harmonic systems require a smaller dynamic range of the ADC, but at the expense of the operational range. For illustration, the same approach of finding the maximum operational range as for linear radars should be repeated for harmonic ones.

In figure 4.8, the received power curves are depicted along with the minimum detectable power of the system, but now for harmonic radars. The simulation included the mathematical model of the harmonic tag written in Matlab [9].

Table 4.5 shows the range for different power budgets, also providing the dynamic range and the corresponding resolution.

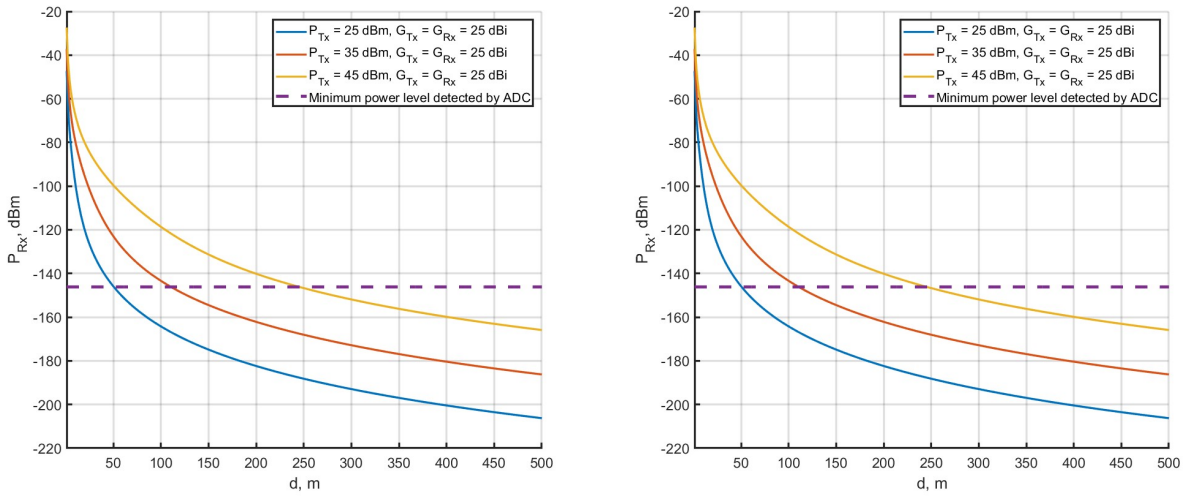


**Figure 4.8:** The received power with respect to the distance to the target for different transmitted power an antenna gains - 15dBi(a),25dBi(b). Also, the minimum power level is readable by the receiver. The intersection of the received power curve and the minimum level is the max. operational range for a certain power budget. Harmonic radar.

| $P_{Tx}$, dBm | $G_{Tx} = G_{Rx}$, dBi | DR, dB | N, bits | max. range, m |
|---|---|---|---|---|
| 25 | 15 | 87.8 | 15 | 26 |
| 35 | 15 | 99.9 | 17 | 49 |
| 45 | 15 | 109.9 | 19 | 112 |
| 25 | 25 | 109.85 | 19 | 76 |
| 35 | 25 | 119.9 | 20 | 163 |
| 45 | 25 | 129.8 | 22 | 365 |

**Table 4.5:** Parameters, and the corresponding DR, resolution, and the maximum operation range for the harmonic system.

In comparison with the linear case, a harmonic radar delivers much lower ranges, although the resolution requirements are not considerably lower. This outcome confirms the poor power efficiency of harmonic FMCW radars. Yet, their advantages open room for applications in heavily cluttered areas.

For harmonic radars, there are 2 ways of defining the cut-off frequencies. One is if third-order highpass characteristics will be used, and the other one implies that a second-order filter with a higher cut-off frequency.

The third-order approach is done in the same manner as for the linear radar: the DR curves with respect to the beat frequency are built along with the DRs for a certain

resolution (see fig. 4.9), and the intersection indicates the required cut-off frequencies. These frequencies are shown in table 4.6. The same resolutions were used as for the linear radar.

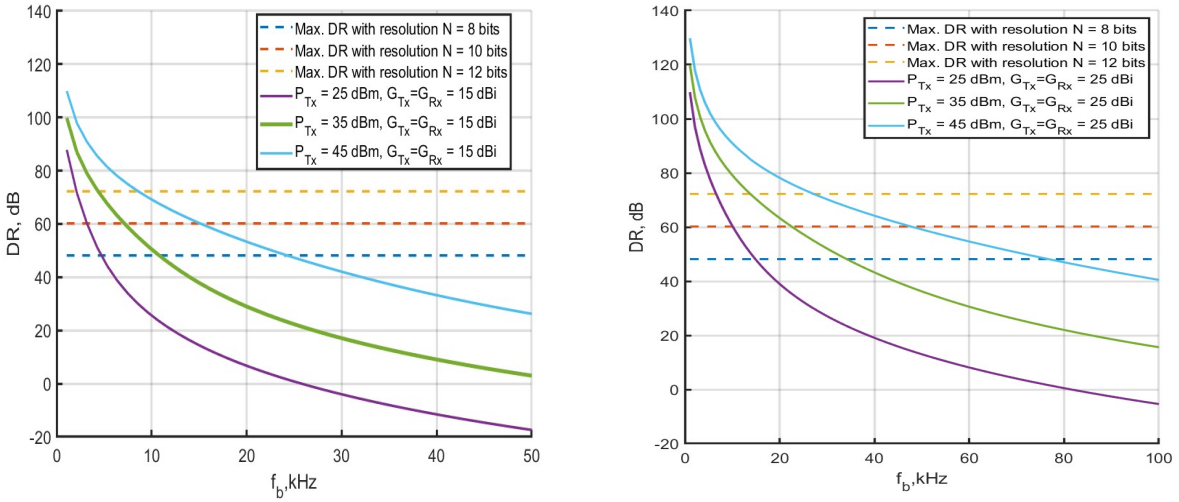


a) b)

**Figure 4.9:** Relations of dynamic ranges versus beat frequency for systems with different transmitted power and antenna gains 15 dBi (a) and 25 dBi (b). The maximum power levels for 8,10,12 bits. The intersections of these levels with the dynamic ranges indicate the cut-off frequencies for HPFs. Harmonic radar

| Power budget \ Resolution, bits | 8 | 10 | 12 |
|---|---|---|---|
| $P_{Tx} = 25dBm, G_{Tx} = G_{Rx} = 15dBi$ | 4.27 | 3.29 | 2.02 |
| $P_{Tx} = 35dBm, G_{Tx} = G_{Rx} = 15dBi$ | 10.67 | 7.20 | 4.34 |
| $P_{Tx} = 45dBm, G_{Tx} = G_{Rx} = 15dBi$ | 23.47 | 15.13 | 8.47 |
| $P_{Tx} = 25dBm, G_{Tx} = G_{Rx} = 25dBi$ | 14.93 | 10.16 | 6.67 |
| $P_{Tx} = 35dBm, G_{Tx} = G_{Rx} = 25dBi$ | 34.13 | 22.21 | 13.86 |
| $P_{Tx} = 45dBm, G_{Tx} = G_{Rx} = 25dBi$ | 76.80 | 47.79 | 27.18 |

**Table 4.6:** Cut-off frequencies for HPF given for certain power budget and for certain ADC resolution. Given in [kHz]

The second approach requires us to expand the large-signal 40dB/decade region on the received power curve with respect to the beat frequency to find the intersection with the power level specifically calculated for the pre-determined dynamic range. The approach was depicted previously in figure 3.3. The same idea is depicted in figure 4.10, but now for the simulated power curves. To be able to distinguish between the different slopes, using a logarithmic frequency axis along with logarithmic power is required.

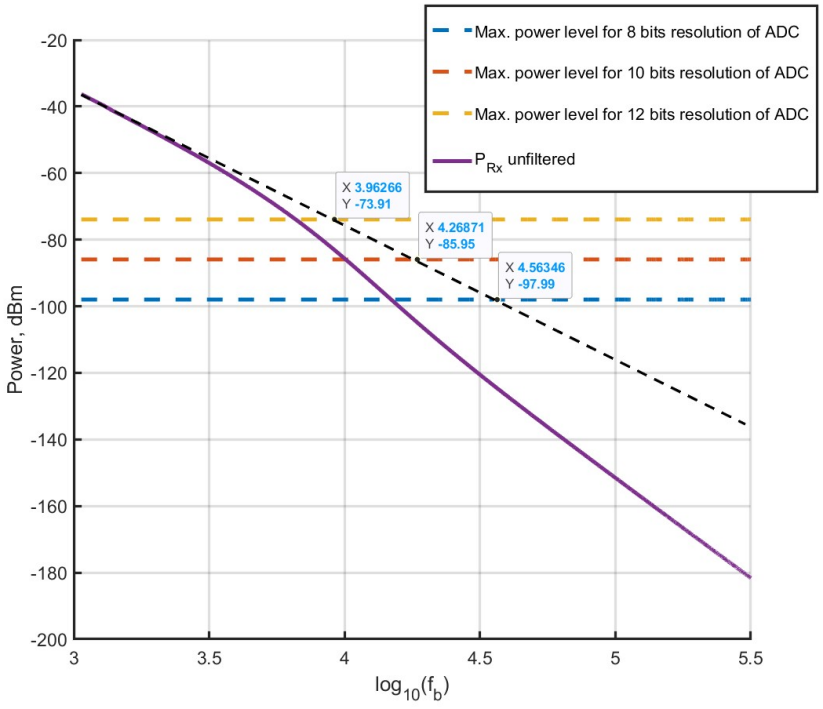


**Figure 4.10:** The process of the calibration of $f_{cut-off}$. The received power ($P_{Tx} = 25dBm$,$G_{Tx} = G_{Rx} = 25dBi$) is plotted with respect to the beat frequency in the logarithmic scale. The large-signal region is extended until it reaches the maximum allowed level for 8,10,12 bits. This is how the cut-off frequency is obtained for the corresponding resolutions.

And table 4.7 shows the new cut-off frequencies for this approach. The data in the table is not given for the lowest power budget ($P_{Tx} = 25dBm$,$G_{Tx} = G_{Rx} = 15dBi$), because with these initial conditions, the power curve already deviates from a perfect 40dB/decade slope at the starting distance of 1 m.

The slope depends on the behavior of the harmonic tag, which is different for different ranges of the incident power. The total output power of the transmitter $P_{Tx} + G_{Tx}$ (in dBm) is the parameter that defines where the transition will occur from 40dB/decade to 60dB/decade. For the lowest power budget, this value is 40dBm, which is apparently enough for the harmonic tag to exhibit non-linear behavior even when located only 1m from the transmitter.

The starting operational distance can be set lower, and the perfect 40dB/decade slope will be visible. However, target ranges below 1 m are likely not of interest, especially for insect tracking.

| Power budget \ Resolution, bits | 8 | 10 | 12 |
|---|---|---|---|
| $P_{Tx} = 35dBm, G_{Tx} = G_{Rx} = 15dBi$ | 19.01 | 9.77 | 5.00 |
| $P_{Tx} = 45dBm, G_{Tx} = G_{Rx} = 15dBi$ | 38.90 | 19.50 | 9.55 |
| $P_{Tx} = 25dBm, G_{Tx} = G_{Rx} = 25dBi$ | 36.30 | 18.62 | 9.12 |
| $P_{Tx} = 35dBm, G_{Tx} = G_{Rx} = 25dBi$ | 60.20 | 33.10 | 15.80 |
| $P_{Tx} = 45dBm, G_{Tx} = G_{Rx} = 25dBi$ | 120.23 | 61.66 | 30.20 |

**Table 4.7:** Calibrated cut-off frequencies for HPF given for certain power budgets and for certain ADC resolutions. Given in [kHz]

Finally, the filter can be applied to the harmonic radar. Figure 4.11 shows how the power curve is affected by a third-order filter transfer function. As can be observed, the IF signal coming from closer $d^{-4}$ ranges, and, therefore, corresponding to a smaller $f_b$, will not be attenuated severely for small power budgets. However, for larger power, the cut-off frequency of the filter is located further, thus the attenuation of the large-signal region will become much more considerable. This happens because the over-attenuated large-signal region's slope can be up to 20dB/decade, and the attenuation grows drastically for higher cut-off frequencies.

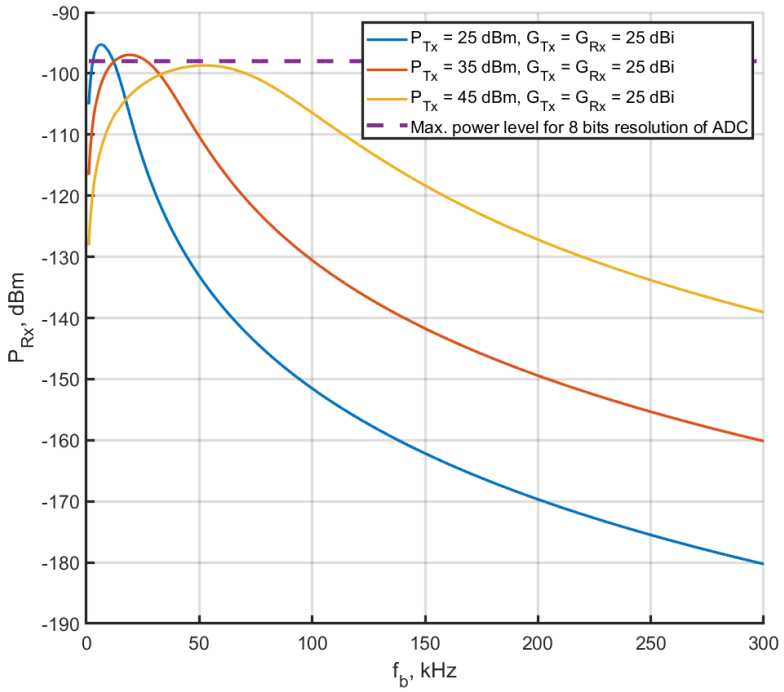


**Figure 4.11:** $P_{Rx}$ vs. $f_b$ for the filtered received signal. The filter is third-order. The data is provided for the resolution of 10 bits, and for three different power budgets.

Another way is to use a second-order filter. The approach is the following: the large-signal region in the logarithmic plot (see figure. 4.10 ) is extended and the intersection with the maximum power level will show what $f_c$ is needed.

The result of this approach can be seen in figure 4.12a. It can be observed that the dynamic range is within the boundaries, and the signal strength for closer ranges is preserved at the highest possible level. Also, if one looks closely at this figure, it can be seen that for the transmitter output power ($P_{Tx}$+$G_{Tx}$) of 50 dBm, the large-signal region already gets very small. For the lowest power budget ($P_{Tx} = 25dBm$,$G_{Tx} = 15dBi$, $G_{Rx} = 15dBi$), when the output power is even smaller, the large signal region will be out of sight in the considered bandwidth. As mentioned, a third-order filter can be applied in this case. On top of that, since the power budget is small, over-attenuation will not be considerable. The figure 4.12b is similar to 4.11. It shows how the filters affect the power curves of different power budgets and for one specified resolution. As can be observed, it looks similar to figure 4.6, which corresponds to applying a second-order HPF to a linear FMCW radar.

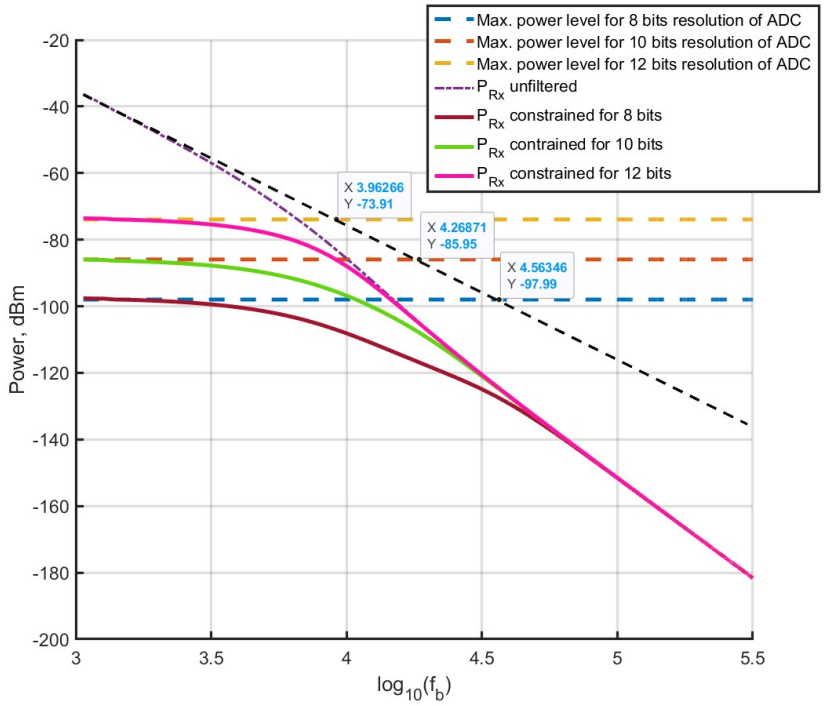


a)

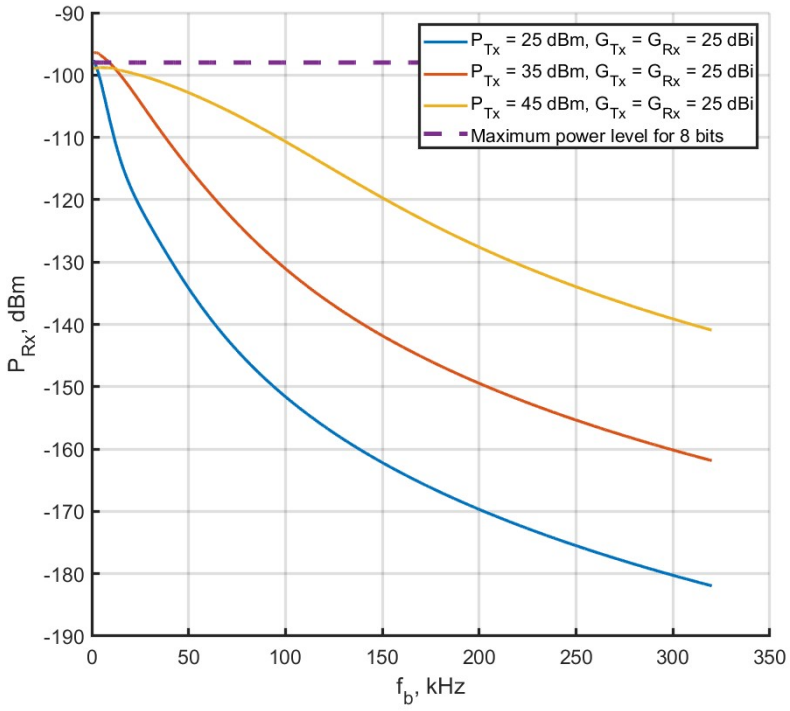


b)

**Figure 4.12:** a)$P_{Rx}$ vs. $f_b$ for the filtered received signal in dB scale. The filter was second-order and the frequencies were calibrated. Parameters: $P_{Tx} = 25dBm$,$G_{Tx} = G_{Rx} = 25dBi$. b) A similar figure to figure 4.11. Given for 3 power budgets and for the ADC resolution of 8 bits.

# Chapter 5

# Conclusion

In this research, the main objective was to find how applying highpass filters as FGC can reduce the required dynamic range of the ADC in FMCW harmonic radars. A comparison had to be made with conventional FMCW radars. With a lower dynamic range, the resolution of the ADC will be lower, and the cost of the ADC will be thus reduced, which is useful for low-cost applications.

Overall, FGC is a capable technique for the dynamic range reduction. The main challenge was the varying path loss that was proportional either to the negative fourth or to the sixth power of distance for incident power levels of the harmonic tag. In comparison to a conventional FMCW radar, for which a second-order highpass characteristic is always applied, the filter order for a harmonic radar depends on the transmitted power and the antenna gains. For higher values of these parameters, a second-order filter with the calibration of the cut-off frequency is more suitable, and for lower values, a third-order highpass filter is applicable.

# Bibliography


[1] “Continuous-wave radar.” [Online]. Available: https://en.wikipedia.org/wiki/Continuous-wave_radar

[2] G. Storz and A. Lavrenko, “Compact low-cost fmcw harmonic radar for short range insect tracking,” in *2020 IEEE International Radar Conference (RADAR)*, 2020, pp. 642–647.

[3] H. Kasahara, T. Moriyama, Y. Yamaguchi, and H. Yamada, “An equivalent sensitivity time control circuit for fm-cw radar,” *Electronics and Communications in Japan (Part I: Communications)*, vol. 80, no. 6, pp. 1–7, 1997. [Online]. Available: https://onlinelibrary.wiley.com/doi/abs/10.1002/%28SICI%291520-6424%28199706%2980%3A6%3C1%3A%3AAID-ECJA1%3E3.0.CO%3B2-O

[4] S. H. Jung, S. G. Kim, W. S. Choi, H. H. Kim, H. G. Kim, and Y. S. Eo, “High dynamic range ku-band cmos transceiver ic for fmcw radar application,” in *2017 IEEE MTT-S International Microwave Symposium (IMS)*, 2017, pp. 1415–1417.

[5] A. Lavrenko and J. Cavers, “Two-region model for harmonic radar transponders,” *Electronics Letters*, vol. 56, no. 16, pp. 835–838, 2020.

[6] Q. Chaudhari, “FMCW Radar Part 1 – Ranging,” https://wirelesspi.com/fmcw-radar-part-1-ranging/, [Online; accessed 30-June-2024].

[7] B. Colpitts and G. Boiteau, “Harmonic radar transceiver design: miniature tags for insect tracking,” *IEEE Transactions on Antennas and Propagation*, vol. 52, no. 11, pp. 2825–2832, 2004.

[8] Y. Wu and J. Linnartz, “Detection performance improvement of fmcw radar using frequency shift,” in *Proceedings of the 32nd WIC Symposium on Information Theory in the Benelux, Brussels, Belgium*, 2011, pp. 1–8.

[9] A. Mogilnikov and A. Lavrenko, “On the modelling and evaluation of harmonic tags,” in *IEEE International Symposium on Antennas and Propagation*. IEEE, 2024, in pres.

[10] “Butterworth filter design.” [Online]. Available: https://nl.mathworks.com/help/signal/ref/butter.html

[11] S. Kong, C. Hu, R. Wang, F. Zhang, L. Wang, T. Long, and K. Wu, “Insect multifrequency polarimetric radar cross section: Experimental results and analysis,” *IEEE Transactions on Geoscience and Remote Sensing*, vol. 59, no. 8, pp. 6573–6585, 2021.